Available online www.jsaer.com

***Journal of Scientific and Engineering Research*, 2019, 6(1):9-22**

Research Article

ISSN: 2394-2630
CODEN(USA): JSERBR

Identification of Petroleum Reservoir Characteristics using 3D Seismic & Log Data in Agbada Field in Niger Delta

Mgbonta B. Ogenna*, Etim D. Uko, Iyeneomie Tamunobereton-ari

Department of physics, Rivers State University, P.M.B 50, Port Harcourt, Nigeria

Abstract Petrophysical evaluation and seismic interpretation of "Agbada field" Onshore Niger Delta basin, was carried out using 3D seismic and log data with an aim to identify petroleum reservoir charateristics in the study area. The work focused on using instrumentation methods to identify reservoirs in sedimentary basins. RMS amplitude extraction, Structural and stratigraphic interpretation was done on the seismic sections while petrophysical analysis and lithologic interpretation was done with well logs. The gross-sand thicknesses range from a minimum of 122 feet to maximum of 500 feet for the AGBD_05, 04 and _01 wells. Net sand thicknesses range from 46 feet to 410 feet, net HC thickness ranges from 25 feet to 120 feet. Three hydrocarbon bearing sands were identified with a good porosity ranging from 22.6% to 26.6%, Sw values ranging from 19.8% to a maximum of 46.8% for the sands calculated. The total STOOIP was estimated to be 45.13 MMbbl. The three reservoirs were ranked using average results of petrophysical parameters. Res_III was found to be more prolific while Res_I was found to be least prolific within Agbada field. Drill-well opportunities occurs in the area marked as prospect. The Faults that was mapped and seen on the time structural map include growth structures, synthetic faults, and antithetic faults. The three horizons (Res_I, Res_II, and Res_III) were mapped and used to understand the stratigraphic nature of the study area. Result shows that the three reservoirs holds a considerable volume of hydrocarbon enough to make a positive business decision.

Keywords 3D seismic, Petrophysical analysis, fault, Porosity, Amplitude extraction

1. Introduction

One of the primary requirements for the occurrence of an oilfield is the availability of reservoirs. A reservoir can be defined as a subsurface pool of hydrocarbons contained in a porous and permeable formation capable of storing and transporting hydrocarbons in economic quantities. Reservoirs can either be conventional or unconventional. Conventional reservoirs are either siliciclastic or carbonate in nature while unconventional reservoirs range from shales to fractured basement. The type of reservoirs present in an area is usually a function of the depositional process that have occurred over time within the basin. The search for hydrocarbons was initially easy, humans looked for surface seeps which they could harness for daily use. However, when surface supplies became scarce people resorted to digging for hydrocarbons which has now evolved into the drilling techniques of today. Petroleum geologists have learned to look for hydrocarbons in areas where they have been found before as well as similar areas to earlier discoveries. The Niger Delta basin has today evolved from being an exploratory province in the 1950's to becoming a prolific petroleum province in the present [1]. Exploratory work has determined that it has a thick sediment accumulation and geological features favourable for hydrocarbon generation, expulsion and trapping from the onshore region to the deep water region of the basin [2]. Migration of interests of exploration companies into deep water plays as well as deep onshore plays has required adaptation and evolving technologies in order to reduce economic risk. A critical understanding of reservoirs is currently required to adequately extract hydrocarbons from these new frontiers. Careful and

cautious planning is carried out to understand the quality, communication and geometry of reservoirs in order to facilitate production at minimum costs. The identification and characterization of reservoirs requires a proper understanding of depositional systems as well as integration of different datasets in order to define the reservoir model [3]. The analysis of any sedimentary environment in the search for hydrocarbons, depends on two basic types of information. One is derived from direct observation of the rocks themselves — from outcrops, cores, and well cuttings. The second type is indirect, being generated by instrumentation: wire-line logs (including dipmeter) and seismic surveys. The petroleum geologist is, however, primarily concerned with the subsurface and therefore key stratigraphic horizons may not be exposed at the surface. This study focus on using instrumentation methods to identify reservoirs in sedimentary basins.

1.1. Location and Geology of the Study Area

The Agbada field (Fig. 1) is located in the Niger Delta Basin, Nigeria. It is the most prolific hydrocarbon bearing basin in Nigeria and the 12th largest in the world. A 3D seismic volume with six (6) well penetrations was provided for this study. Composite suite of logs like gamma ray, resistivity, sonic and density logs as wells as a TDR data was provided.

The Niger Delta (Fig. 2) is considered among the world's best studied delta provinces. The Niger Delta, situated at the apex of the Gulf of Guinea on the west coast of Africa, covers an area of about 75 000 km² [4]. Basement tectonics related to crucial divergence and translation during the late Jurassic and Cretaceous continental rifting probably determined the original site of the main rivers that controlled the early development of the Delta [5]. The Cenozoic development of the delta is also believed to have taken place under approximate isostatic equilibrium [6]. The main depocenter is thought to have been at the triple junction between the continental and oceanic crust where the delta reached a main zone of crustal instability [7-8]. The Niger Delta is a large arcuate delta of the destructive, wave-dominated type and is composed of an overall regressive clastic sequence which reaches a maximum thickness of about 12 km in the basin center [6].

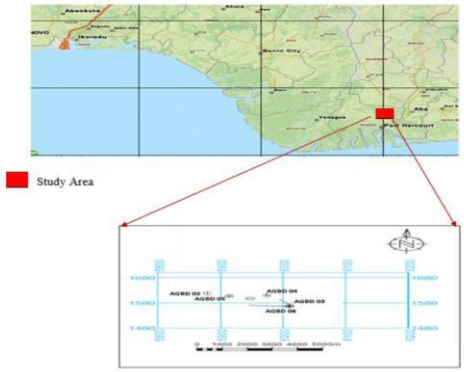

Figure 1: Location and base map of the study area showing seismic lines and well

There are three lithostratigraphic units recognized in the Niger Delta namely Akata, Agbada and Benin Formations. The Niger Delta comprises a 'coarsening upward' sequence of Tertiary clastics over mainly Cretaceous sediments, forming a thick sedimentary cover as the deltas of the Niger and Benue Rivers developed [9]. These sediments constitute the prolific petroleum systems of the Niger Delta. Basal marine shales, probably the main source rocks, are overlain by mainly unconsolidated delta-front reservoir sands, which exhibit excellent reservoir properties, with porosity of 40% and permeability up to 5,000 mD [10]. Intercalating shales function both as additional source rock and as seals, and are overlain by sands thick enough to have created sufficient overburden for maturation [11]. Migration pathways were provided by the laterally extensive sand units.

The oil found in the Niger Delta is a 'sweet' low-sulphur crude, typically in the 35-45° API range, paraffinic and waxy. The identity of the major source rocks has long been the subject of debate, primarily because there is no single rich source rock in the conventional sense, and while the assumption is that hydrocarbons are sourced from the Tertiary, there is some evidence for an older, Mesozoic origin.

The majority of traps in the Delta is structural, with syn-depositional growth-faults, rollover anticlines and collapsed crest structures all featuring [12-13]. Complexity increases offshore, as shale tectonism and diapirism

due to rapid sedimentation and over-pressure, is common. In the deep-water delta there is a complex pattern of channels, fan lobes and turbidites on a grand scale. Stratigraphic traps are more likely on the flanks of the basin and in ultra-deep-water.

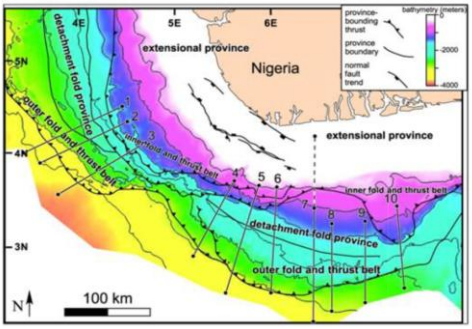

Figure 2: Location map of the Niger Delta showing the major structural provinces

2. Materials and Methods

The data used in this study was gotten from Shell Petroleum Development Company with the appropriate permission from DPR. The data consists of migrated 3-D seismic, checkshot data and a suite of well logs. The well log data were used for petrophysical analysis in order to calibrate the rock properties to seismic attribute which would help in determining sand distribution. The checkshot data was used to calibrate the sonic log for seismic to well tie and also to depth convert the surface map to the depth domain from the time domain.

The software used for this work includes Petrel 2014, MS Excel, and Geographix.

2.1. Petrophysical Analysis

2.1.1. Volume of Shale Estimation

In other to estimate the volume of shale, the gamma ray index is calculated first [14] using the equation:

$$I_{GR} = \frac{GR_{\log} - GR_{\min}}{GR_{\max} - GR_{\min}} \quad (1)$$

Where I_{GR} = gamma ray index

GR_{log} = gamma ray reading of the formation

GR_{max} = maximum gamma ray reading

GR_{min} = minimum gamma ray reading

The volume of shale, which is the percentage of shale contained in a reservoir, was calculated using Dresser Atlas [15] formula for Tertiary rocks:

$$V_{Sh} = 0.083\left(2^{3.7*I_{GR}} - 1\right) \quad (2)$$

2.1.2. Estimation of total and Effective Porosity

Porosity is the percentahe of voids to the total volume of rock. The formation density log, neutron, and sonic logs were used to estimate the total and effective porosity. According to Rider.M [16], and [17], the most accepted and more accurate porosity is that which is calculated from the bulk density log. The formation porosity (Ø) was determined by inputting the values of the rock matrix density, ρ_{ma}, the fluid density, ρ_f, and the bulk density, ρ_b, obtained from the density log within each reservoir into the equation.

$$\phi_T = \frac{\rho_{ma} - \rho_b}{\rho_{ma} - \rho_f} \quad (3)$$

Where ρ_{lma} = matrix density; ρ_b = Bulk density read directly from the log; ρ_f = the fluid density; ϕ_T =Total porosity.

The average rock density in the sandstones research reports is 2.66gcm^{-3} and the average rock density in the shale is 2.65gcm^{-3}. The fluid density depends on the type of fluid the well encountered (water or hydrocarbon). The hydrocarbon density was calculated from composition and phase considerations, oil = 0.80 gcm^{-3}. The water density used was 1gcm^{-3}.

The effective porosity (ϕ_e) was calculated using the equation given below:

$$\phi_e = (1 - V_{Sh})\phi_T \quad (4)$$

2.1.3. Determination of Water Saturation

For the estimation of fluid saturation in any reservoir, the formation factor (F) is calcuated first by using the equation:

$$F = \frac{a}{\phi^m} \quad (5)$$

where *a* = is a constant value for the turtosity factor; *m* = is the cementation exponent.

For this study, 0.62 and 2.15 were used for the turtosity factor and the cementation exponent respectively for unconsolidated Tertiary rocks of the Niger delta. The water saturation in the reservoir is calculated by using the Archie's [18] equation for water saturation given as:

$$S_w = \left(\frac{FR_w}{R_T}\right)^{\frac{1}{n}} \quad (6)$$

where n = is the saturation exponent (2); R_w = is the formation water resistivity; R_t = is the true resistivity (resistivity of uninvaded zone).

2.1.4. Estimation of irreducible water saturation and permeability

This is the lowest amount of water that can be present within a reservoir. It was derived by taking a minimum baseline along the water saturation log. It can also be estimated by using the equation:

$$S_{wir} = \sqrt{\frac{F}{2000}} \quad (7)$$

Where *F* = is the formation factor

Permeability values for the reservoir zones were estimated by use the Tixier's equation which relates permeability to irreducible water saturation [19]:

$$K = \left[\frac{250 * \phi^2}{S_{wir}}\right]^{1/2} \quad (8)$$

Where K = permeability in millidarcies; ϕ = effective porosity as a bulk volume fraction; S_{wirr} = irreducible water saturation.

2.1.5. Net-to-Gross Ratio

This is a key petrophysical parameter that measures the amount of reservoir sands within the entire lithostratigraphic package. It helps in reservoir quality appraisal and it is a very critical reservoir scale property for the characterisation of reservoirs and field development. It could be high in the well scale and low on seismic scale, thus it is scale dependent [20].

$$\frac{Net}{Gross} = \frac{h}{H} \quad (9)$$

Where H= gross sand; h= net reservoir.

3. Results and Interpretation

3.1. Stratigraphic Correlation

Correct interpretation of well logs is important to any reservoir identification and characterization. According to [21], log correlation gives the basis for the determination of reservoir architecture and geometry. All three wells analysed had gamma ray and resistivity logs which were used for the correlation exercise. Initially, the total length of logs was loaded into the Petrel software and viewed together. The correlation revealed a very thick sequence of high resistivity sands in the shallow zones that was easy to pick in each well. This was interpreted to be the freshwater sands of the Benin Formation. These sands decreased in average thickness from the

AGBD_02 well in the northwest progressively to the AGBD_06 in the southeast. At the base of these sands is a relatively thick shale layer, varying from a minimum of 20 feet in AGBD_03 well to a maximum of about 95 feet on average in AGBD_02. This thick shale layer is the first in a sequence of sand and shale inter-layers of variable thickness within which all the wells attained TD. This last sequence was interpreted as part of the hydrocarbon-bearing Agbada Formation. After establishing the gross stratigraphic correlation of the Formations penetrated by the wells, a close-up correlation was made on the hydrocarbon-bearing levels (Fig 3). At these levels, there is a general thickening of the sands from the east to the west. The shales, on the other hand, thin generally to the east.

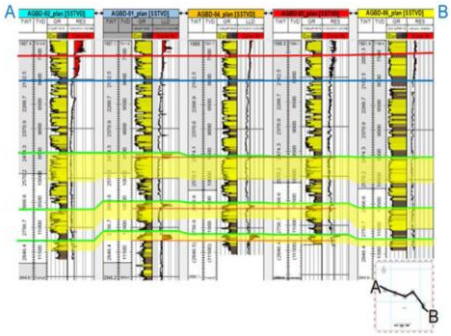

Figure 3: Correlation panel showing the delineated sand units in the wells

3.2. Seismic/Well Ties

The Sonic log from AGBD_04 was calibrated with TDR data from same well and combined with density log to produce a reflection coefficient. Synthetic seismogram was generated by convolving the reflection coefficient with wavelet derived from the seismic data.

The synthetic seismogram was used for tying the well data and seismic data. This tie formed the bases for picking events which corresponds to the tops of sands of interest for interpretation. The synthetic seismogram generated revealed that Agbada wells have a good time depth tie with a trough to trough and peak to peak match. Well-to-seismic tie revealed that the mapped hydrocarbon bearing reservoirs lie on a trough of the rollover anticlines on the seismic section. Fig. 4 shows the synthetic seismogram of AGBD_04 and the mapped well tops. Three seismic horizons were mapped in total, corresponding to Res_I, Res_II and Res_III. These Horizons were chosen because they are hydrocarbon-bearing. The characteristics of the seismic events selected for interpretation are listed in Table 2.

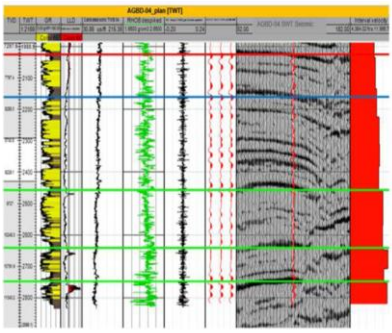

Figure 4: Seismic-to-well tie showing the three reservoir sands (Res_I, Res_II and Res_III)

Table 2: Characteristics of seismic events selected for interpretation

Horizn Name	Seismic Event	Event Character
Res_I	Trough	Generally good, but discontinuous in some areas
Res_II	Trough	Fair to Good but discontinuous in some areas
Res_III	Trough	Fair to Good

3.3. Horizon/Fault Interpretation and Mapping

The seismic interpretation exercise was initiated on the 3D Inline 59691 in the south-western portion of the block. The mapped faults were used to capture the structural styles and controls relative to sediment supply rate in the accommodation spaces created by the movement of the faults (Fig. 4 & 5). Inline 59691 passes right through the AGBD_04 well location. An initial line spacing of every eight dip lines and every sixteen strike lines was utilized for the seismic interpretation. This was eventually changed to every four dip lines and every eight strike lines to firm up the prospects. Prior to this, tops of sands that were hydrocarbon-bearing had already been posted in the wells and these top picks had been posted on the seismic sections using the available velocity data.

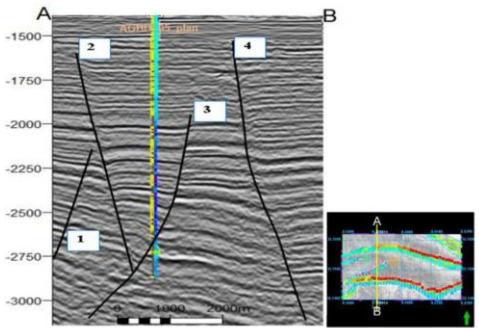

Figure 4: Seismic inline 59691 Interpretation of Faults showing structural pattern with time slice at -2200ms showing W–E trending faults

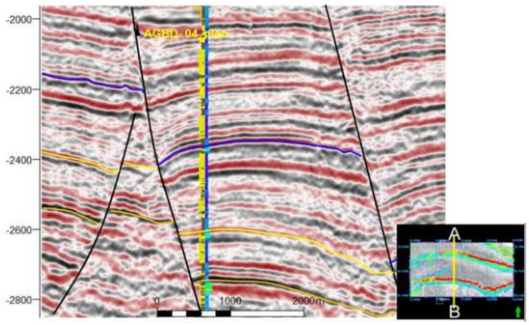

Figure 5: Seismic inline 59691 showing the mapped fauls and horizons

The faults were first identified and interpreted on the dip lines to set up the structural framework of the area. The structure of the field indicated major growth faults and antithetic faults which forms the major structural trap type identified in the Niger Delta by [6].

Strike lines and time-slices were used later to firm up the positioning and continuity of the faults picked. The fault segments were then correlated to individual fault planes. Next, the horizons were picked throughout the volume and the picked faults were used to generate fault polygons.

The seed-picked horizons were then interpolated, constrained by the final fault polygons to make the time structure maps. The derived time-depth relationship for AGBD_04 was then used to convert the time data into depth data still in Petrel.

Time Maps were created for the areas covered by 3D seismic (Figs. 6, 8 & 10). These maps were later converted to depth map with RMS amplitude attribute overlay (Figs. 12, 13 & 14).

3.3.1. Res_I Horizon Level

The time map at the Res_I horizon level shows 3 distinct microstructural units or fault blocks separated by 2 major, approximately West-East trending normal faults –B and G located north to south respectively (Fig. 6). Five other minor normal faults, striking parallel to the above-mentioned, were picked across the horizon, two of which dip to the southwest and one of which is an antithetic, dipping to the north.

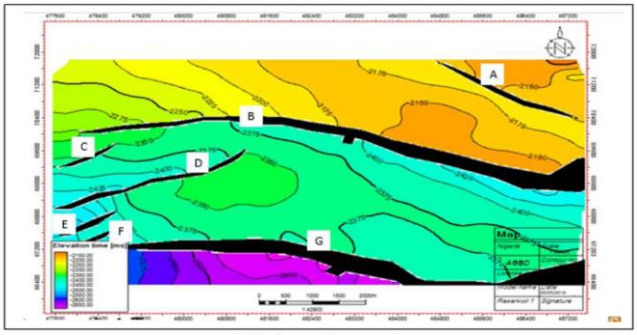

Figure 6: Time map for Reservoir I

Within the Central Fault Block is a 3-way dip-closure closing against the normal and antithetic fault (Faults B and D respectively) to the West and with a culmination at about 2350 milliseconds.

Fig. 7 shows an RMS amplitude extraction map of 20ms window for Res_I horizon level. This amplitude map shows the distribution of high and low amplitude across the horizon. It also indicates fluid content, lithology, high and low porosity and permeability areas. The high amplitude/bright spots (red, yellow and green colour) regions at the central to western part of the central fault block of the map indicates the presence of hydrocarbon. This bright spots corresponds to the rollover structure of field.

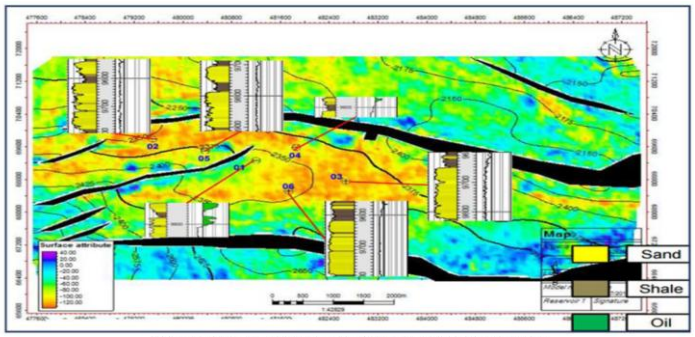

Figure 7: Time Map showing RMS Amplitude Extraction for Reservoir I

3.3.2. Res_II Horizon Level

The time map at the Res_II horizon level shows 3 distinct microstructural units or fault blocks separated by 2 major, approximately West-East trending normal faults –C and F located north to south respectively (Fig. 8). Five other minor normal faults, striking parallel to the above-mentioned, were picked across the horizon, two of which dip to the southwest and one of which is an antithetic, dipping to the north.

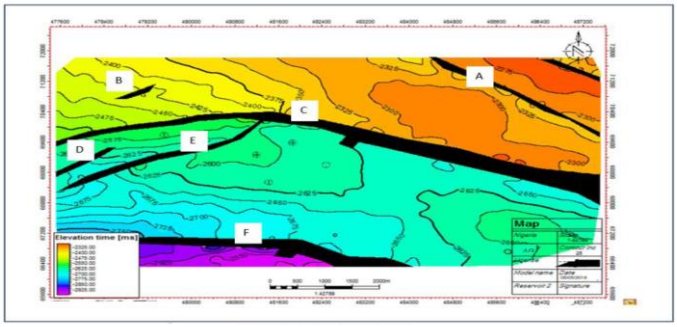

Figure 8: Time map for Reservoir II

There exists a 3-way dip-closure closing against the antithetic fault (Fault F) to the West and with a culmination at about 2600 milliseconds. Further to the south-Eastern part of the map and still within the Central Fault Block is another 3-way dip-closure closing against the normal fault to the South and with a culmination at about 2600 milliseconds.

Fig. 9 shows an RMS amplitude map for Res_II horizon level. The bright spots observed at the western and southern part of the central fault block of the map indicates the presence of hydrocarbon and corresponds to the rollover structure of field.

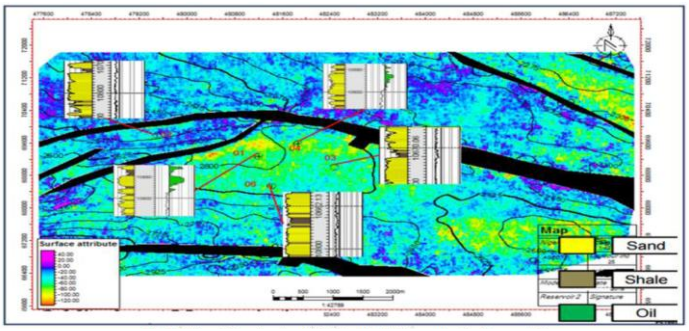

Figure 9: Time Map showing RMS Amplitude Extraction for Reservoir II

3.3.3. Res_III Horizon Level

The time map at the Res_III horizon level shows 3 distinct microstructural units or fault blocks separated by 2 major, approximately West-East trending normal faults –D and F located north to south respectively (Fig. 10). Six other minor normal faults, striking parallel to the above-mentioned, were picked across the horizon, two of which dip to the southwest and one of which is an antithetic, dipping to the north.

In the North-Eastern part of the northern fault block shows a 3-way-closure closing against faults A and D with a culmination at about 2500 milliseconds.

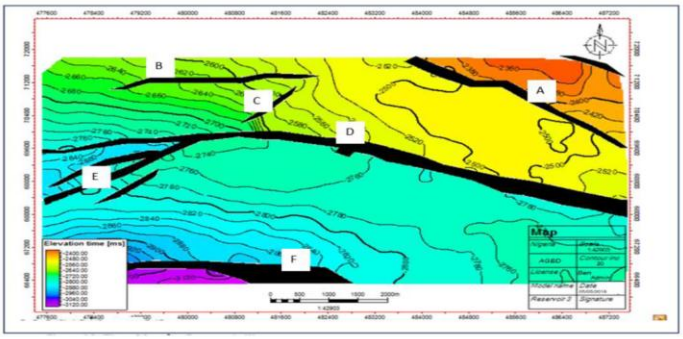

Figure 10: Time map for Reservoir III

Fig. 11 below shows the RMS amplitude map for Res_III horizon level. The bright spots observed at the North-Eastern fault block and at the central part of the central fault block of the map indicate the presence of hydrocarbon and both corresponds to the rollover structure of field.

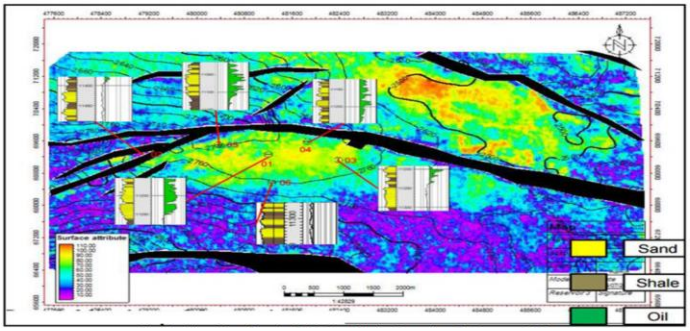

Figure 11: Time Map showing RMS Amplitude Extraction for Reservoir III

3.4. Reservoir Description

In the study area, three hydrocarbon-bearing sands, Res_I, Res_II and Res_III were identified and were all penetrated by the AGBD wells and these reservoirs were all hydrocarbon-bearing. In addition, only AGBD_04

and _01 has TDR data. As a result, fluid contact depths from AGBD_04 only was used to construct the depth maps and calculate net-pay thicknesses and ultimately estimated volumes of hydrocarbon in place.

Res_I Sand

The Res_I sand was penetrated by all the six wells at different subsea depths. The AGBD_05, _04, and _01 wells encountered the sand in the Western part of the Central Fault Block at a subsea depths of 9680ft, 9560ft and 9500ft respectively. Fig.12 shows the Central Fault Block structure as essentially a large combination dip and fault-closed structure with a crestal thickness of about 90ft somewhere to the West. The resistivity data in the wells were used to interpret the presence of oil in the reservoir and the Neutron-Density data was used for identifying fluid contacts. The reservoir is interpreted as having an oil-water-contacts at different well points. AGBD_05, _04 and _01 wells saw an oil-water-contact (OWC) at 9705ft, 9575ft and 9605ft subsea respectively.

The reservoir characteristics of the Res_I sand in the study area are relatively good. The Res_I sand in AGBD_04 well saw a gross sand of 390 feet, but a net sand of only 335 feet, giving a net-to-gross ratio of just 0.86. The net oil found/pay thickness was 35 feet, average porosity was 26.6% and average water saturation was 33% (Table 3).

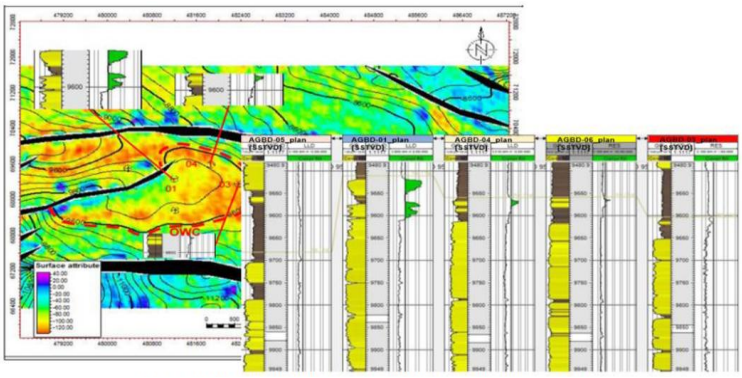

Figure 12: Depth structure Map with RMS Amplitude overlay for Reservoir I

Table 3: Summary of petrophysical analysis of AGBD_05

Well 5									
SAND	**TOP (TVDSS)**	**BASE (TVDSS)**	**HC TYPE**	**GROS SAND (ft)**	**NET SAND (ft)**	**NTG**	**NET HC (ft)**	**CONTACT (TVDSS)**	**CONTACT TYPE**
RES I	9680	9890	OIL	210	45	0.21	25	9705	OWC
RESII	10616	10977	OIL	361	163	0.45	27	10643	OWC
RES III	10988	11110	OIL	122	68	0.56	115	11111	ODT

Res_II Sand

The Res_II sand was penetrated by all the six wells at different subsea depths. The AGBD_04, _01, and _05 wells encountered the sand in the Western part of the Central Fault Block at a subsea depths of 10540ft, 10520ft, and 10616ft, respectively (Table 3 – 5). Fig. 13 shows the Central Fault Block structure as essentially a large combination dip and fault-closed structure with a crestal thickness of about 120ft somewhere to the West. The resistivity data in the wells were used to interpret the presence of oil in the reservoir and the Neutron-Density data was used for identifying fluid contacts. The reservoir is interpreted as having an oil-water-contacts at different well points. AGBD_05, _04, and _01 wells saw an oil-water-contact (OWC) at 10643ft, 10590ft and 10580ft subsea respectively.

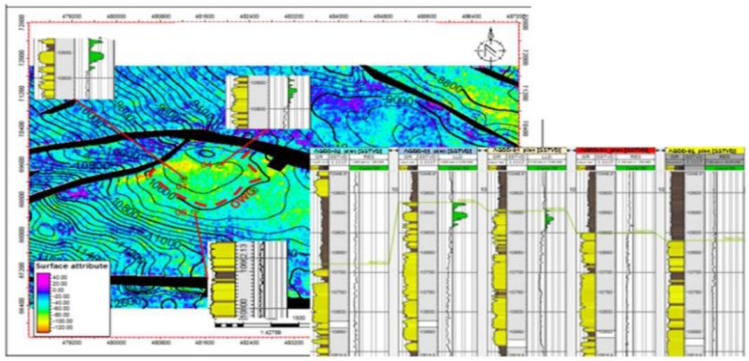

Figure 13: Depth structure Map with RMS Amplitude overlay for Reservoir II

The reservoir characteristics of the Res_II sand both from the seismic and well logs are good. The Res_II sand at AGBD_04 saw a gross sand of 343 feet, but a net sand of only 261 feet, giving a net-to-gross ratio of 0.76. The net oil found/pay thickness was 40 feet, average porosity was 25.7% and average water saturation was 31.1% (Table 3 – 5).

There are currently no wells drilled in the South-Eastern part of the Central Fault Block, within which a 'lead' have been identified (fig. 14).

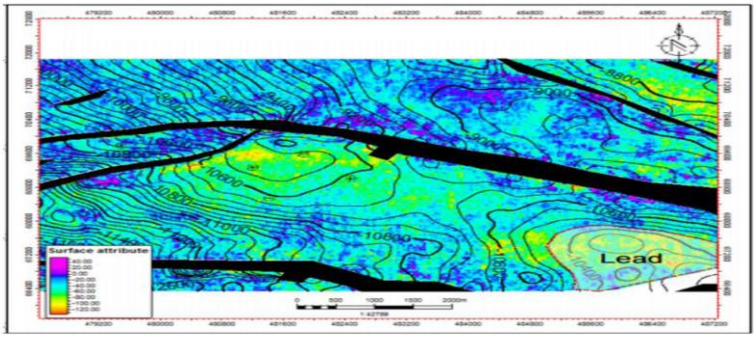

Figure 14: Depth structure Map with RMS Amplitude overlay showing identified Lead in Reservoir II

Res_III Sand

The Res_III sand was penetrated by all the six wells at different subsea depths. The AGBD_05, _04, and _01 wells encountered the sand in the Western part of the Central Fault Block at a subsea depths of 10988ft, 11120ft, and 11150ft respectively (Table 3 – 5). Fig. 15 shows the Central Fault Block structure as a large combination dip and fault-closed structure with a crestal thickness of about 110ft. The resistivity data in the wells were used to interpret the presence of oil in the reservoir and the Neutron-Density data was used for identifying fluid contacts. The reservoir is interpreted as having an oil-water-contacts at different well points. AGBD_05, _04, and _01 wells saw an oil-down-to (ODT) at 11111ft, 11240ft, and 11250ft subsea respectively.

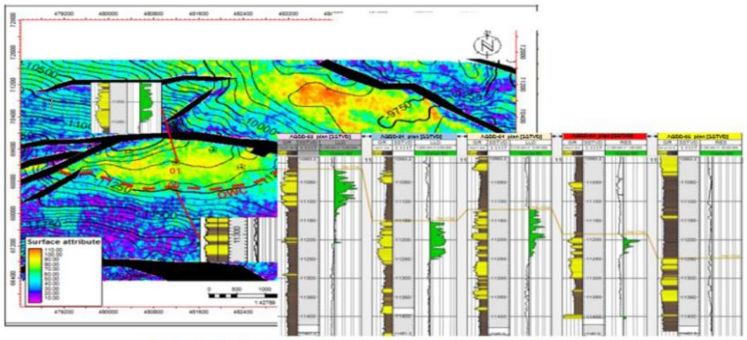

Figure 15: Depth structure Map with RMS Amplitude overlay for Reservoir III

The reservoir characteristics of the Res_III sand in the Agbada field is good. The Res_III sand in AGBD_04 well saw a gross sand of 123 feet, but a net sand of 46 feet, giving a net-to-gross ratio of 0.37. The net oil found was 120 feet, average porosity was 22.9% and average water saturation was 18.1% (Table 3 – 5).

There are currently no wells drilled in the Northern Fault Block, within which a prospect has been recognized. This is shown in Fig. 16 as Prospect. This prospect is a combination dip and fault-closed structure with an estimated thickness of about 110ft.

The reservoir characteristics of the Prospect from the RMS seismic attribute extracted shows a high reflectivity. This indicates that the Prospect is highly porous and permeable. The expected fluid within the area is Gas/oil with gas-oil-contact at 9714ft.

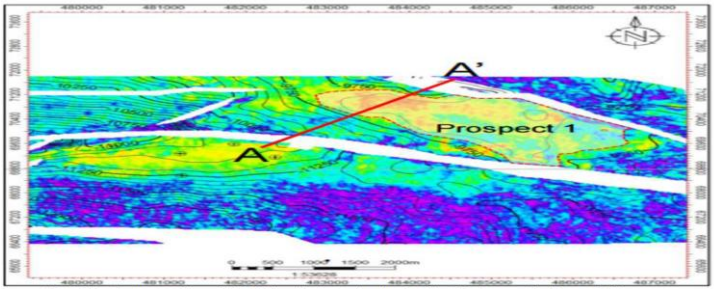

Figure 16: Depth structure Map with RMS Amplitude overlay showing identified prospect in Reservoir III

Table 4: Summary of petrophysical analysis of AGBD_04

Well 4									
SAND	**TOP (TVDSS)**	**BASE (TVDSS)**	**HC TYPE**	**GROS SAND (ft)**	**NET SAND (ft)**	**NTG**	**NET HC (ft)**	**CONTACT (TVDSS)**	**CONTACT TYPE**
RES I	9560	9950	OIL	390	335	0.86	35	9575	OWC
RES II	10540	10883	Gas/OIL	343	261	0.76	40	10570	GOC
								10590	OWC
RES III	11120	11243	OIL	123	46	0.37	120	11240	ODT

Table 5: Summary of petrophysical analysis of AGBD_01

Well 1									
SAND	**TOP (TVDSS)**	**BASE (TVDSS)**	**HC TYPE**	**GROS SAND (ft)**	**NET SAND (ft)**	**NTG**	**NET HC (ft)**	**CONTACT (TVDSS)**	**CONTACT TYPE**
RES I	9500	10000	OIL	500	410	0.82	100	9605	OWC
RES II	10520	10900	OIL	380	250	0.66	70	10580	OWC
RES III	11150	11270	OIL	120	81	0.68	110	11250	ODT

4. Discussion

The hydrocarbon volumes were calculated separately for the three reservoirs in the Agbada field, with their Proven, Probable and Possible hydrocarbon as seen by the AGBD_01 and _04 wells and for the rest of the block covered by seismic, treated as prospects and carried as additional possible hydrocarbon. There were procedural differences in the computation of proven, probable and possible hydrocarbon volumes.

For proven volumes, net pay isopachs were constructed for each hydrocarbon-bearing sand. In Petrel, the areas between the isopach lines of each reservoir or individual unit were planimetered. Using individual well data from petrophysical analysis of AGBD wells (porosity and water saturation) the P10, P50, and P90 values for reservoir parameters were determined. The actual AGBD data represent (P50), (P10), and (P90) are distributions of porosities and water saturations between 17% - 26% and 43% -30% respectively (Tables 6 & 7). The prospects petrophysical data had a distribution of AGBD data for (P10), (P50), and (P90), see details in Tables 6 & 7.

The ratio of the planimetered areas of any two successive isopach lines were determined. Where this ratio is less or equal to 0.5, the pyramidal method was used, otherwise the trapezoidal method was used for the

determination of oil or gas bulk volumes in acre-ft. Using any of the methods above, gross rock volumes were calculated for P10, P50, and P90 respectively (fig. 17).

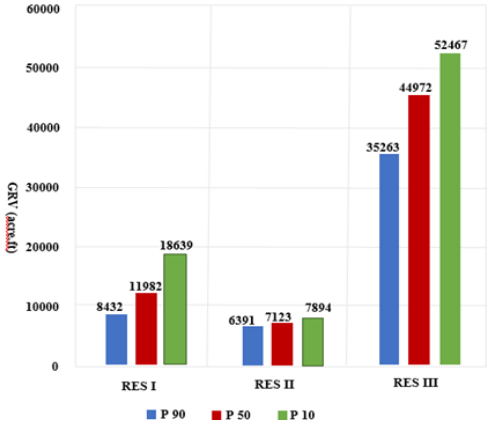

Figure 17: Chart showing the Gross rock volume calculated for the three identified reservoirs

Gross rock volumes calculated above, with respective distributed petrophysical properties (porosity and water saturation) and formation volume factor (FVF) for each interval were used as input data into the Volumetric equations for original oil or gas in place in Stock Tank Barrels of oil and Standard cubic feet of gas (fig. 18). A recovery factor of 0.35 was then applied to original oil calculated above to obtain the un-risked proven reserves for each reservoir.

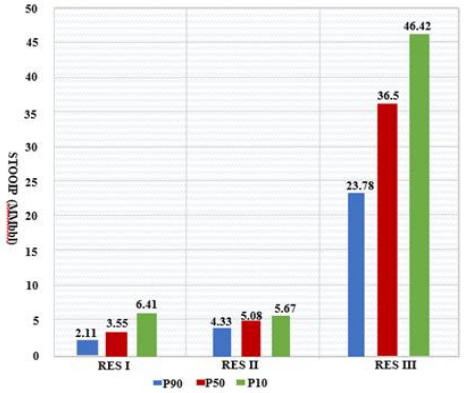

Figure 18: Chart the calculated Stock tank original-oil-in-place for the three reservoirs

For probable volumes, the areas between the oil-up-to (OUT) structured contour line and two times (2X) the net sand thicknesses or to the crystal structure contour line were planimetered. The areas between the oil-down-to (ODT) structured contour line and two times (2X) the net sand thicknesses or to the point of spill were planimetered (for Downdip probable). This was done for every reservoir with probable potential.

The reserves classified as possible was the prospects identified (fig. 15). The entire area enclosed as prospect was planimetered. Using distributed data from electric logs of AGBD wells, (net sand, porosity, water saturation) the P10, P50, and P90 of the gross rock volumes were obtained. Areas calculated above, with respective distributed petrophysical properties (net sand thickness, porosity, water saturation) and 1/FVF for each interval as input data into the Volumetrics software for the calculation of stock tank original oil/gas in place (fig.19).

Figure 19: Chart the calculated Stock tank original-gas-in-place for the identified prospect

For additional input for gas volumes calculations, temperature, pressure and gas gravity were included. Using the method above, original oil and gas in place for P10, P50, and P90 were calculated respectively. Recovery factors of 0.35 and 0.70 were applied to original oil or gas in place respectively to obtain the possible reserves for the prospect.

For the STOOIP calculation, a Bo of 1.50 rb/stb was used. Since no PVT or reservoir condition data was provided, this Bo value was taken from regional trend. The recoverable reserves figure was derived using a recovery factor of 0.35 for oil and 0.70 for gas which similarly is from analogy, for lack of relevant data. Pressure and Temperature values were calculated using water gradient for the corresponding reservoir depth and regional temperature gradient of 1.8 °F per 100 ft respectively. A value of 0.70 was assumed for gas gravity.

Table 6: Summary of petrophysical analysis of (Reservoir I), Agbada field

RES. NAME	NTG (%)	POROSITY φ (%)	SW (%)	Thickness (ft)	Pay
	21.2	26.6	33.4	20	P90
RES_I	66.4	25.2	38.3	27	P50
	80.2	22.6	46.1	38	P10

Table 7: Summary of petrophysical analysis of (Reservoir II), Agbada field

RES. NAME	NTG (%)	POROSITY φ (%)	SW (%)	Thickness (ft)	Pay
	45.8	25.7	31.1	34	P90
RES_II	58.1	25.6	31.3	45	P50
	76.3	25.1	33.2	70	P10

Table 8: Summary of petrophysical analysis of (Reservoir III), Agbada field

RES. NAME	NTG (%)	POROSITY φ (%)	SW (%)	Thickness (ft)	Pay
	37.5	22.9	18.1	98	P90
RES_II	62.9	22.9	19.3	100	P50
	69.3	22.8	19.8	120	P10

5. Conclusion

The 'Agbada' Field is located within an active portion of the Niger Delta Basin that contains 45.13 Mbbls of STOOIP and 453 Mscf of OGIP volumes.

- The Paleocene - Eocene shales of the Akata and Agbada formation serve as source rocks.
- field is separated into 3 fault blocks by major faults.
- The Agbada Field has several vertically stacked reservoirs which occurs along a roll-over anticlinal structures within the fault blocks.
- A total of three different sands are hydrocarbon-bearing in the seismic and AGBD wells logs analyzed. All the hydrocarbon-bearing sands had oil and some portion of Res_III sand is inferred to have gas, based on an overlap observed in the neutron and density logs of the AGBD_04 well.
- The results obtained from both the seismic and well logs data shows a near identical results in the reservoir characteristics of the 'Agbada' Field.
- The gross-sand thicknesses range from a minimum of 122 feet to maximum of 500 feet for the AGBD_05, 04 and _01 wells. Net sand thicknesses range from 46 feet to 410 feet, net HC range from 25 feet to 120 feet. Porosity values range from a minimum of 22.6% to a maximum value of 26.6% while the S_w had values ranging from 19.8% to a maximum of 46.8% for the sands calculated.
- Drill-well opportunities occur to the north of the tested fault block with probable gas accumulations in the area identified as a prospect.

References

[1]. Petroconsultants. (1996). Petroleum exploration and production database: Houston, Texas, Petroconsultants, Inc.

[2]. Klett, T. R., Ahlbrandt, T. S., Schmoker, J. W. & Dolton, J. L. (1997). Ranking of the world's oil and gas provinces by known petroleum volumes: U.S. Geological Survey Open-file Report-97-463, CD-ROM.

[3]. Beka. F.T., and Oti, M.N. (1995). The distal offshore Niger Delta: frontier prospects of a mature petroleum province, in, Oti, M.N., and Pastma, G., eds., Geology of Deltas: Rotterdam, A.A. Balkema, p. 237-241.
[4]. Webber, K. J., and Daukoru, E. M. (1975). Petroleum Geology of the Niger Delta: Proceedings of the ninth world Petroleum Congress, volume 2, Geology: London, Applied Science Publishers, Ltd.
[5]. Hospers, J. (1965). Gravity Field and Structure of the Niger Delta, Nigeria, West Africa. Geological Society of American Bulletin: Vol. 76, pp. 407-422.
[6]. Doust, H., and Omatsola, E. (1990) Niger Delta, in Edwards, J.D., and Satogrossi, P.A., eds., Divergent/passive Margin Basins, AAPG Memior 48: Tulsa, American Association of Petroleum Geologists p. 239-248.
[7]. Kulke, H. (1995). "Nigeria": Kulke, H., (ed.), Regional Petroleum Geology of the World. Part II: Africa, America, Australia and Antarctica: Berlin, Gebruder Borntraeger, pp.143-172.
[8]. Ekweozor, C. M., and Daukoru, E. M. (1994). Northern delta depobelt portion of the Akata-Agbada petroleum system, Niger Delta, Nigeria.
[9]. Kaplan, A, Lusser, C. U., Norton, I. O. (1994). Tectonic map of the world, panel 10: Tulsa, American Association of Petroleum Geologists, scale 1:10,000,000.
[10]. Weber, K. J. (1971). Sedimentological aspects of oil fields in the Niger delta, Geologie en Mijnbouw, vol. 50, pp. 559–576.
[11]. Adikwu, S.O, Oluoma, C. F, Oleson,. J. and Obaje, E. C. (2017). 3D Seismic Interpretation and Petrophysical Analysis of "Olu Field" Onshore Niger Delta
[12]. Coffen, J. A. (1984). Interpreting seismic data: Penwell Publishing Company, Tulsa Oklahoma. pp. 39-118.
[13]. Ejeh, I. O. (2010). Sedimentary Fill Modeling: Relationships to Sequence Stratigraphy and Its Implications for Hydrocarbon Exploration in the Niger Delta, Nigeria. The Pacific Journal of Science and Technology, V. 11. No. 1, p. 502-509.
[14]. Asquith, G. And Charles R. G. (1982). Basic Well Log Analysis for Geologists. AAPG Special volume. Pub. Id: A093 (1982), pp. 91.
[15]. Dresser Atlas. (1979). log Interpretation Charts. Houston .Dresser Industries, Inc., p: 107.
[16]. Rider, M. (2006). The geological interpretation of well logs. Progress Press Co. Ltd, Malta, p. 43-67.
[17]. Horsfall, O. I., Uko E. D. and Tamunobereton-ari, I. (2013). Comparative analysis of sonic and neutron-density logs for porosity determination in the Southeastern Niger Delta Basin, Nigeria.
[18]. Archie, G. E. (1950). Introduction to Petrophysics of reservoir rocks. AAPG Bulletin, Tulsa, 34 (5): 943-961.
[19]. Aigbedion, I., and Hafiz, A. (2016). Evaluation of Hydrocarbon Prospect of Fareed Field, Western Niger-Delta, Nigeria: Journal of Geography, Environment and Earth Science International 7(4): 1-8, 2016; Article no. JGEESI.29113.
[20]. Sonny Inichinbia, Peter O. Sule, Halidu Hamza, and Aminu L. Ahmed. (2014). Estimation of net-to-gross of among hydrocarbon field using well log and 3D seismic data. IOSR Journal of Applied Geology and Geophysics (IOSR-JAGG), PP 18-26, Volume 2, Issue 2 Ver. II'.
[21]. Coates, G. R., and Denoo, S. (1981). The producibility answer product: Schlumberger Technical Review, v. 29, no. 2, p. 54–63.